Potential overall heat exposure reduction associated with implementation of heat mitigation strategies in Los Angeles

D. J. Sailor, J. Anand & L. Kalkstein

ONLINE FIRST

International Journal of Biometeorology

ISSN 0020-7128

Int J Biometeorol
DOI 10.1007/s00484-020-01954-5

International Journal of Biometeorology
https://doi.org/10.1007/s00484-020-01954-5

SPECIAL ISSUE: INDOOR BIOMETEOROLOGY

Potential overall heat exposure reduction associated with implementation of heat mitigation strategies in Los Angeles

D. J. Sailor[1,2] · J. Anand[2,3] · L. Kalkstein[4]

Received: 17 March 2020 / Revised: 5 June 2020 / Accepted: 9 June 2020

Abstract

We analyzed two historical extreme heat events in Los Angeles to explore the potential of increasing vegetative cover and surface solar reflectance (albedo) to reduce total exposure (indoor and outdoor) to dangerously hot conditions. We focus on three population subgroups, the elderly, office workers, and outdoor workers, and explore the extreme case where each subgroup does not have functioning air conditioning in their residences. For each heat event, we conducted atmospheric model simulations for a control case and four mitigation cases with varying levels of increased albedo and vegetation cover. Simultaneously, we conducted building simulations of representative residential buildings that lacked mechanical air conditioning. These simulations factored in both the indirect cooling effects associated with neighborhood implementation of mitigation strategies and the direct effects of high albedo roofing on the individual buildings. From both the atmospheric and building models, we exported hourly values of air temperature and dew point temperature, and used this information in combination with various scenarios of occupant behavior to create profiles of individual heat exposure. We also gathered heat-mortality data for the two heat events and developed a synoptic climatology-based relationship between exposure and excess mortality. This relationship was then applied to the scenarios in which albedo and canopy cover were increased. The results suggest that improvements in indoor thermal conditions are responsible for a sizable portion of the health benefit of large-scale implementation of heat mitigation strategies.

Keywords Heat-related health · Individually experienced temperatures · Heat exposure · Heat mitigation · Indoor environmental quality

Background

In the USA, on average, extreme heat causes more deaths each year than hurricanes, lightning, and tornadoes combined (CDC 2018). Heat is also implicated in numerous physical and mental health illnesses (Pedersen 2015; Vassos et al. 2016). Climate change is expected to increase both the frequency and magnitude of heat waves, and, as cities grow, the local effects of urbanization are anticipated to create a warming on par with global climate change (Krayenhoff et al. 2018).

However, while most heat-related health analyses focus on outdoor ambient conditions, most urban residents spend more than 85% of their time in indoor environments (Klepeis et al. 2001). Investigations of heat-related deaths during heat-wave events report that decedents were more likely to succumb to heat in their own home ([CDC] Centers for Disease Control and Prevention 2013; Fouillet et al. 2006), and that poor, socially isolated, and elderly populations are at the greatest risk of heat-related mortality (Fouillet et al. 2006; Kaiser et al. 2007; Semenza et al. 1996). A growing field of inquiry centers around the concept of personal exposure and individually experienced temperatures (e.g., Kuras et al. 2015; Sailor et al. 2016; Kuras et al. 2017). As a result, there is an increasing recognition that estimates of indoor and outdoor conditions

Electronic supplementary material The online version of this article (https://doi.org/10.1007/s00484-020-01954-5) contains supplementary material, which is available to authorized users.

✉ D. J. Sailor
dsailor@asu.edu

1 School of Geographical Sciences and Urban Planning, Arizona State University, Tempe, AZ, USA

2 Urban Climate Research Center, Arizona State University, Tempe, AZ, USA

3 School for Engineering of Matter, Transport and Energy, Arizona State University, Tempe, AZ, USA

4 Applied Climatologists, Inc, Marco Island, FL, USA

Published online: 19 June 2020

must be considered when exploring potential to mitigate heat-related illness and death (O'Lenick et al. 2019; Sailor 2014).

We hypothesize that the heat exposure benefits of urban heat mitigation strategies are substantially different when considering indoor and outdoor conditions, and the ways in which vulnerable populations move between and operate in these environments. This is accomplished in a case-study modeling effort that links mesoscale atmospheric modeling of heat mitigation with whole building simulations of representative building stock. Mesoscale model simulation of heat mitigation strategies has been a popular mode of investigation of the regional-scale efficacy of highly reflective materials and urban vegetation for decades (e.g., Oke 1976; Akbari et al. 1990; Sailor 1998; Salamanca et al. 2012; Morini et al. 2018). Modeling of the building energy and indoor effects of rooftop implementation of highly reflective materials has also seen a great deal of attention in the literature (e.g., Hildebrandt et al. 1998; Shen et al. 2011; and Baniassadi et al. 2018). The present study combines these two scales of modeling to explore the indoor and outdoor exposure conditions for urban residents using Los Angeles, CA, as a case study. Simulations explore these conditions during two historical extreme heat events (EHE) under control conditions as well as under scenarios of heat mitigation. These results are then linked to implications for adverse health outcomes.

Methods

Mesoscale modeling

Regional-scale simulations of the effects of large-scale heat mitigation deployment were conducted using the urbanized version of the Weather Research and Forecasting (WRF, v3.8.1) model (Chen et al. 2011). All simulations were conducted at the county level using the 40-category land cover data available from the National Land Cover Database (NLCD) and four nested grids (see Fig. 1) with resolutions of 1, 3, 9, and 27 km. The analysis uses model output from the finest resolution (1 km) domain, centered on downtown Los Angeles.

The single layer urban canopy model of Kusaka was used along with default geometries for parameterized urban canyons in low density residential, high density residential, and commercial land use areas. The low, medium, and high intensity development categories used in the modeling are based on fraction of impervious surface as defined in the National Land Cover Database (NLCD) and described in Homer et al. (2015). Low intensity urban land cover corresponds to areas with a mix of constructed materials and vegetation, with impervious surfaces accounting for 20 to 49% of total cover (typically single-family housing units). The medium intensity urban land cover includes areas with 50 to 80% impervious surface cover (typically higher density housing). The high intensity classification is for areas with 80 to 100% impervious cover (typically commercial and industrial areas). The shadowing effects of buildings on ground-level surfaces were included by changing the default value of the shadow calculation control parameter in the model source code.

All simulation cases were provided atmospheric initial and boundary conditions from the NCEP North American Reanalysis (NARR) 3-hourly atmospheric data. Key model physics parameterizations included the Rapid Radiative Transfer Model (RRTM) with the Dudhia shortwave radiation scheme, Monin-Obukhov (Janjic Eta) similarity scheme for the surface layer, the Mellor-Yamada-Janjic Turbulent Kinetic Energy (TKE) scheme for boundary layer physics, and the Noah Land Surface Model.

We present results for simulations focused on two historical EHEs. The first heat event, July 22–25, 2006, was a relatively hot and humid event, while the second, August 26–29, 2009, was a much drier event. Both events were defined by the presence of oppressive air masses that encompassed the entire region. The July 2006 event was dominated by "moist tropical plus (MT+)" air mass conditions. The maximum and minimum air temperatures during the hottest day of this event were 39 and 25 °C, respectively (at Burbank Airport). The average dew point temperature was just over 18 °C and the midday relative humidity hovered around 30–50%. The average wind speed was 10.7 m/s. The August 2009 event also included some "dry tropical" (DT) days, with the hottest day reaching a maximum and minimum air temperature of 41 and 19 °C, respectively. This event had an average dew point temperature of just over 2 °C and the midday relative humidity hovered around 10–15%. The average wind speed was 6.3 m/s. See Sheridan and Kalkstein (2004) for a discussion of the synoptic climatology of MT+ and DT air masses. The presence of both extremely hot air masses most often leads to negative health outcomes among the general population, especially for the elderly, homeless, and poor (Kalkstein et al. 2019). All simulations were conducted with a focus on the 4-day heat event episode. However, each simulation was initiated 7 days prior to the period of interest to allow for model spin-up.

Common mitigation strategies include use of high solar reflectance (albedo) rooftop and street surfaces and increasing the vegetated canopy cover throughout the city (e.g., Stone et al. 2012). The present study focuses on these approaches. High albedo modifications were implemented by modifying the roof and road albedo values within the urban parameters input file of WRF. Vegetation increases were implemented by suitably modifying the urban vegetation coverage variables in the vegetation parameterization input file for WRF. A control case (case 0) and four mitigation cases were simulated as summarized in Table 1. The mitigation cases were identified as realistic pathways based on current policies, strategies, and targets being developed and implemented within the city of

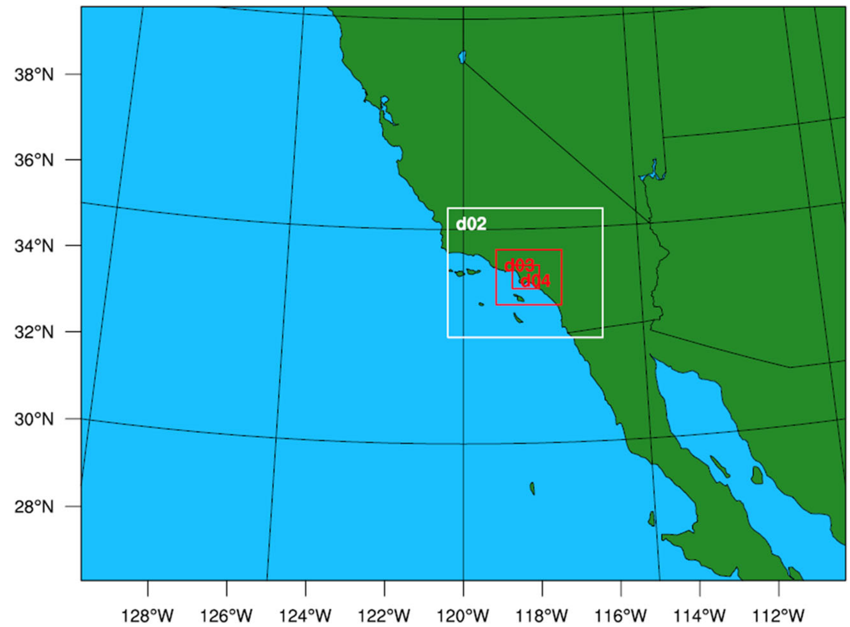

Fig. 1 Nested grid representation of the Los Angeles basin. The innermost domain uses 1 km resolution grid cells covering an area of 150 by 150 km

Los Angeles (Garcetti 2019). They are consistent with the level of modification required to achieve desired city-wide urban cooling goals of 1–2 °C (Sailor 1995; Santamouris 2014). Thus, the mitigation cases include an option focused on increasing albedo (case 1), a case focused on increasing canopy cover (case 2), and cases that combine moderate/high albedo and moderate/high canopy cover (cases 3/4).

For each simulation, hourly results for 2 m dry bulb air temperature and dew point were averaged over all urban grid cells in the finest domain and exported for use in assessing outdoor thermal exposure and for driving the building scale models to ultimately assess indoor exposures.

Indoor environment modeling methods

The EnergyPlus software (Crawley et al. 2001) was used to calculate the indoor thermal conditions for each case. We limited our analysis to single-family residential buildings, but explored two vintages of buildings. Specifically, building archetypes were based on the International Energy Conservation Code (IECC) single-family Los Angeles reference model (Mendon et al. 2013). One building represents homes constructed after the year 2000 (post-2000), and the other represents buildings constructed before 2000 (pre-2000). See the supplemental information and Table S1 for details. For each mitigation case, the rooftop material albedo was adjusted based on Table 1. Changes in road albedo and in canopy cover were not directly integrated in the building models. Rather, the indirect effects of all mitigation strategies were implemented through modifications of the weather files used to drive the building models and the driving weather conditions were modified as discussed below.

Occupant behavior is crucial to this analysis in two respects. First, during warm weather, it is typical that occupants of buildings without air conditioning will attempt to use windows to provide natural cooling when appropriate. However, actual window operating behavior varies substantially. To examine the role of common window operating strategies on indoor exposure, we developed five different cases as summarized in Table 2. Each building model includes 8 windows of dimensions 2.72 by 1.52 m. The windows are assumed to be of the casement window type such that "fully open" (FO) corresponds to a window opening of 4.13 m^2, or the horizontal sliding type such that "half open" (HO) corresponds to a window opening of 2.07 m^2. The S01 and S02 cases correspond to window operation scenarios that take into account safety

Table 1 Canopy cover and albedo parameters used in the control and mitigation cases

Case #	Description	Canopy cover (%)	Pavement albedo	Rooftop albedo
0	Control case	16.6	0.10	0.17
1	Low canopy, high albedo	20	0.35	0.45
2	High canopy, low albedo	40	0.20	0.27
3	Moderate canopy and albedo	30	0.25	0.37
4	High canopy and albedo	40	0.35	0.45

Table 2 Window operation scenarios and characteristics

Operation case	Description	Subgroup using schedule	Area of opening for each window (m^2)	Time open
CW	Closed window	---	None	Never
FO	Fully open evening	---	4.13	6 pm to 10 pm
HO	Half open evening	---	2.07	6 pm to 10 pm
SO1	Safety open overnight	Indoor and outdoor workers	0.23	7 pm to 9 am
SO2	Safety open always	Elderly	0.23	Always

concerns regarding burglary and fall risk. Specifically, the conventional maximum recommended opening width of windows, considering fall risk, is 0.15 m (King et al. 2001) which is roughly the size of a child's head.

In this study, individual exposure analysis focuses on three population subgroups: the elderly, office workers, and outdoor workers. Keeping in mind that this analysis focuses on residents in buildings without air conditioning, the closed window (CW) window operation case is considered the extreme case, as it will result in the warmest indoor conditions. While uncommon, in some cases, concerns over crime or other limitations preclude the operation of windows. In general, when indoor temperatures are higher than outdoor, occupants tend to open their windows. We hypothesize that the most common cases of window operation are SO1 and SO2, with the SO2 case being typically followed by the elderly, as they spend most of their time indoors. On the other hand, we assume that the SO1 case is most typically followed by the working population, including office and outdoor workers.

In addition to building characteristics (geometry, materials, and schedules), the whole building simulation models require specification of ambient weather conditions. As the most common building simulation scenario is for the purpose of sizing mechanical equipment and estimating building energy consumption, the weather in such modeling is usually represented by "typical meteorological year" (TMY) files that seek to capture the most common weather patterns throughout the year. For the purpose of simulating specific historical episodes, the actual conditions for the period of interest (and the antecedent 2 weeks) must be used in place of the TMY data. For this analysis, the typical meteorological year (TMY3) weather is used. The TMY3 files are provided by the Building Technologies Office of the U.S. Department of Energy. To incorporate the selected two historic EHEs, we have replaced the dry bulb temperature, and dew point temperature in the TMY3 file as needed. For the control cases, this required simply replacing TMY data with observations (for the EHE and antecedent 2 weeks). For the August 26–29 2009 heat event, we replaced these data with observations from the KCQT weather station (USC Campus in Downtown) for the period August 1 to August 30. For the July 22–25 2006 heat event, because of missing data, we replaced only from July 11 to July 31. Nevertheless, for both EHEs, the model spin-up requirements have been met, as demonstrated in the model validation data presented below.

The weather files for the mitigation cases were modified by adding hourly perturbations of dry bulb temperature and dew point to the control simulation weather file. For the 4-day period of each EHE, these perturbations were simply the hourly differences between the control and mitigation runs. For the 7-day period before the EHE, weather data were pre-conditioned by first defining the average hourly diurnal profile of perturbations from the EHE event and then subtracting this average profile from the TMY data for the pre-conditioning period.

While there is no single thermal comfort metric that is appropriate for exposure to combined indoor and outdoor climates, the Heat Index (Rothfusz 1990), which takes into account dry bulb temperature and humidity, can be used as a screening metric to assess the magnitude and extent of exposure that each population subgroup is expected to experience during the control conditions and under conditions of the heat mitigation cases. To create such a heat exposure metric, we note that the National Weather Service defines four regions in their assessment of likelihood of heat disorders with prolonged exposure or strenuous activity. These are caution (27 < HI < 32 °C), extreme caution (32 < HI < 41 °C), danger (41, HI < 54 °C), and extreme danger (HI > 54 °C). For the purposes of assessing heat exposure in this study, we focus only on hours when the heat index is above the minimum threshold for the extreme caution category. Specifically, we calculate heat exposure using a metric that is qualitatively similar to the concept of cooling degree days, used for assessing cooling demand in buildings. This metric, which we refer to as "excessive heat hours" (EHH), accounts for both the duration and magnitude of conditions above the extreme caution threshold. It is defined by:

$$\mathrm{EHH} = \sum_{h=1}^{24} (HI_h - 32) * \delta_h \text{ where } \delta_h = \begin{cases} 1 \textit{ for } (HI_h - 32) > 0 \\ 0 \textit{ for } (HI_h - 32) < 0 \end{cases} \quad (1)$$

where the EHH metric is for a single representative day within the EHE, and HI is the Heat Index (in °C) defined by:

$$HI = -8.78 + 1.61*T + 2.34*R - 0.15*T*R - 1.23*10^{-2}*T^2 - 1.64*10^{-2}*R^2 + 2.21*10^{-3}*T^2*R + 7.25*10^{-4}*T*R^2 - 3.58*10^{-6}*T^2*R^2 \quad (2)$$

where T is dry bulb temperature in °C, and R is relative humidity in percentage.

Estimating heat-related mortality

To estimate heat-related mortality for each of the EHE, we employ the synoptic climatology approach outlined in Kalkstein et al. (2018). The recent use of this methodology has suggested that, by utilizing highly reflective materials on roofs and pavement within the urban area, we can actually change the character of some oppressive air mass (DT and MT+) days during intense heat waves to something less likely to produce negative health outcomes. Daily mortality data were obtained from the National Center for Health Statistics, which included information on the cause, place (county), date of death, age, and race ([NCHS] National Center for Health Statistics 2018). These data are then used to develop a heat mortality model that uses as input the ambient air temperature and dew point at four specific hours each day (5 am, 11 am, 5 pm, and 11 pm local time).

Total daily mortality across the cities' standard metropolitan statistical area was summed for each day and then standardized to account for demographic changes in the population characteristics during the period (Sheridan et al. 2009). The mortality for each day is expressed as a variation above or below a standardized baseline.

After standardization, mean anomalous daily mortality, or the number of deaths above what would be expected, was calculated for each air mass type. In both Chicago and Boston, the DT and MT+ air masses were associated with the greatest increase in mortality over baseline levels. However, not all days within these air masses demonstrate elevated mortality. So, a stepwise linear regression was developed for each city to determine which variables accounted for this mortality variation. The independent variables used in our analysis were meteorological (e.g., morning and afternoon temperature, dew point, wind speed, and cloud cover), persistence-oriented, or the number of consecutive days of the air mass occurring during the EHE, and seasonal (time of season), since EHEs in June have shown to be more deadly than similar EHEs in September. This statistical procedure resulted in an algorithm for each city containing statistically significant independent variables. It was used to estimate mortality during particular EHEs both in reality and under modeled conditions.

The developed model can then be applied to WRF-model output for the control case as well as each mitigation case. This approach establishes a baseline estimate of the potential reduction in mortality resulting from changes in outdoor conditions alone. This analysis is not directly applicable to subdivided populations, or populations moving between indoor and outdoor environments, but does provide a baseline, that, when paired with estimates of how subpopulation exposures change under mitigation scenarios, can shed light on the potential importance of including both indoor and outdoor exposure estimates in future studies of heat-related morbidity and mortality.

Results

Mesoscale model performance was validated against observations from local airports. The model was successful in replicating diurnal temperature trends with a root mean square error of approximately 2.0 °C for both extreme heat events modeled (see Supplementary Materials Fig. S1). The diurnal profile of model error exhibited no systematic biases. Having confirmed the performance of the baseline (control) cases for the atmospheric model, we then simulated 4 additional mitigation test cases as summarized in Table 1. The appropriateness of the building model and occupant behavior (window use) assumptions are discussed in the Supplementary Materials section.

For each simulation case, hourly near surface temperature and humidity data were extracted and corresponding hourly differences (control–mitigation case) were calculated. These perturbations were then applied to the underlying weather files for use both in driving the building simulation models and as outdoor conditions for estimation of exposure.

Mitigation strategy effects on indoor and outdoor environments

Figure 2a shows the reduction in outdoor air temperature relative to the control run for each mitigation case. During daytime hours, the high albedo case performs better than the high canopy cover case. However, the high canopy cover case performs better at night. This is to be expected as the energy-balance effects of the high albedo case scale with the incident solar radiation intensity, while the canopy cover cooling effects are influenced both by solar radiation and by ambient temperature and humidity. A similar result was observed by Lee et al. (2009), who compared air temperature observations between a vegetated park and the nearby surroundings. As a result, case 4, which both has high albedo and high canopy cover, performs best throughout the diurnal cycle. Average reductions in ambient air temperature and increases in dew point temperature are summarized in Table S2.

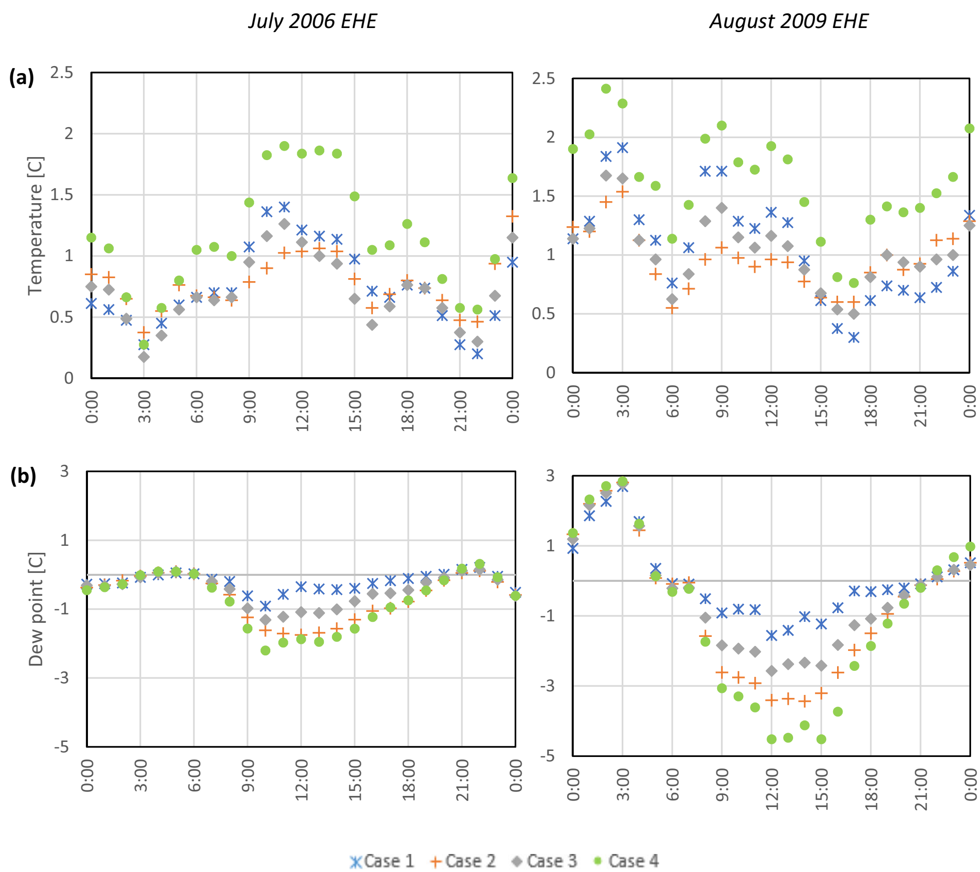

Fig. 2 Reduction in outdoor **a** air temperatures and **b** dew point temperatures for the control and four mitigation case scenarios for July 24 of the 2006 heat event (first column) and August 29 of the 2009 heat event (second column)

To compare the impact of these mitigation strategies, we have used the extreme case of the CW building model. The indoor air temperature reduction (Fig. 3) follows a similar pattern to the outdoor air temperature reduction profiles of Fig. 2. The cases with high albedo perform well during the daytime, while high canopy cover performs better at night. Average indoor temperature reduction and dew point temperature increase throughout the EHE period are summarized in Table S3.

Effect of mitigation strategies on heat exposure

The results for the three subgroup populations show that, in the absence of functioning air conditioning, the elderly have a similar heat exposure as outdoor workers. In fact, between noon and 6 PM, the elderly actually experience considerably higher heat exposure than office workers, and marginally higher heat exposure than outdoor workers (see Fig. 4). Maintaining closed windows between 8 AM and 6 PM elevates the indoor temperature considerably above the outdoor temperature, exposing outdoor and office workers to excessively high temperatures upon returning to their homes each evening.

Figures 5 and 6 show results of the control case and each mitigation strategy for the three population subgroups (elderly, outdoor workers, and office workers). In all population subgroups, mitigation case 4, with high albedo and canopy cover, shows the greatest reduction in outdoor dry bulb temperature. In the case of the elderly population subgroup, there is a peak temperature reduction of 1.22 °C and 1.89 °C for the July 2006 and August 2009 EHE, respectively. The second-best strategy for reducing heat exposure is the high albedo/low canopy of case 1, with peak temperature reduction of 0.80 °C and 1.38 °C respectively, for the July 2006 and August 2009 EHE. A similar pattern is observed in other subgroups as well. In the case of outdoor workers, the peak temperature reduction corresponding to case 4 is 1.46 °C for the July 2006 EHE and 2 °C for the August 2009 EHE. Office workers are in conditioned indoor environments during the hours of peak temperatures for an EHE. However, for the control case, they are still exposed to a maximum of 36 to 37 °C. Thus, mitigation strategies are relevant for office workers as well. Interestingly for the selected day, peak heat exposure happens at the same time for both outdoor workers and office workers, resulting in a similar peak reduction result. Other mitigation cases show a similar result for office workers (around 0.8 °C and 1.46 °C for the July 2006 and 1 °C and 2 °C for the August 2009 EHE respectively) in terms of peak

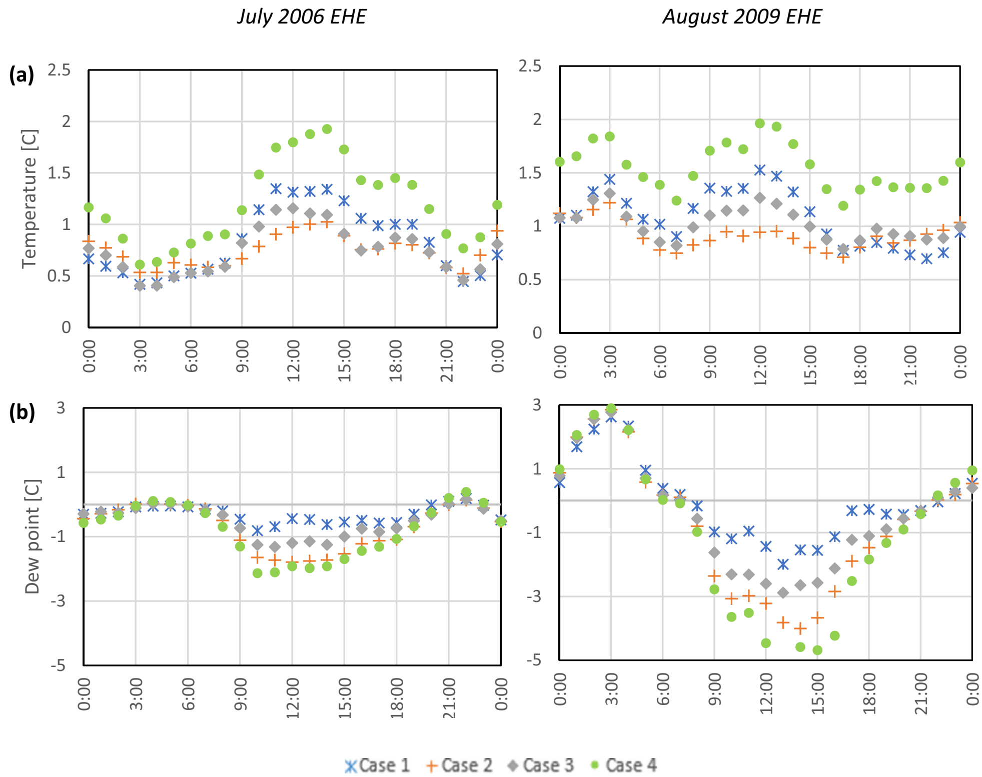

Fig. 3 Reduction in indoor **a** air temperatures and **b** dew point temperatures for the control and four mitigation case scenarios, of closed window building model (CW), for July 24 of the 2006 heat event (first column) and August 29 of the 2009 heat event (second column)

temperature reduction. Increase in canopy cover did not play much of a role in reducing peak heat exposure; even case 3 (moderate canopy and albedo) has greater reduction in peak temperature than case 2 (high canopy and low albedo) for all subgroups.

Health implications of mitigation strategies

The heat-related health impacts of mitigation strategies can be estimated from two perspectives. Traditional approaches only consider changes in outdoor thermal conditions. In this

Fig. 4 Representative diurnal profiles for **a** air temperature and **b** dew point exposure for each of these 3 populations for July 24 of the 2006 heat event (first column) and August 29 of the 2009 heat event (second column)

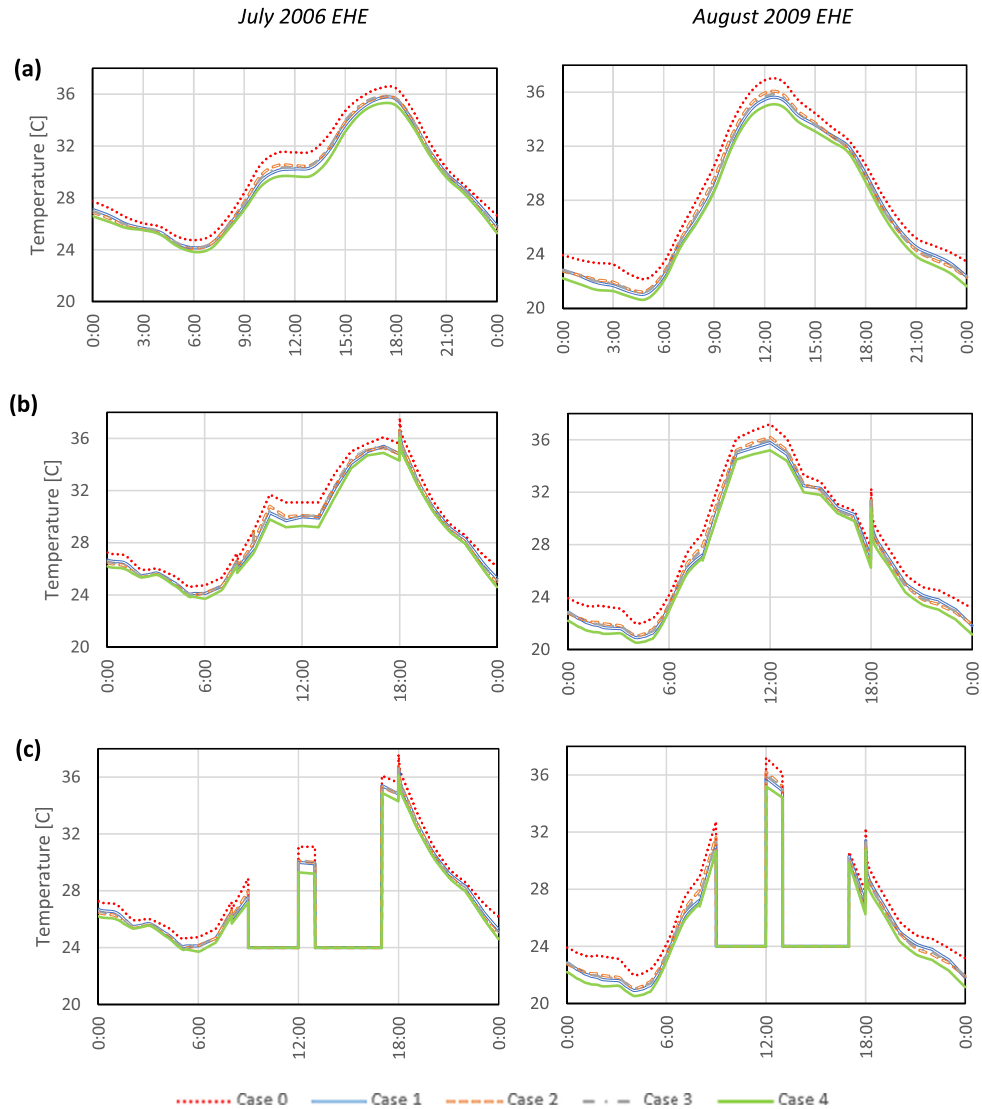

Fig. 5 Typical diurnal profiles for dry bulb temperature of **a** elderly, **b** outdoor worker, and **c** office worker for July 24 of the 2006 heat event (first column) and August 29 of the 2009 heat event (second column)

analysis, we supplement this approach with one that also considers exposure in indoor environments.

First, we evaluate the role of modified outdoor conditions on heat-related mortality estimates for the four cases on outdoor temperature and dew point conditions for the July 2006 and August 2009 heat events. For the hot, humid MT+ dominated 2006 event, we estimated that about 60 extra deaths occurred across Los Angeles county due to the excessive heat. Using the case 4 scenario, we estimated that 49 deaths would have occurred, a savings of 11 lives in this singular heat event, representing an 18% reduction in mortality. In fact, heat-induced mortality decreased by double digits for three of the four mitigation case scenarios (13% for case 1, 9% for case 2, 12% for case 3, 18% for case 4). Air mass changes, from oppressive MT+ to a non-oppressive MT air mass, occurred on two of the five heat event days for cases 1, 2, and 3, and for three of the days in case 4, an impressive result.

The August 2009 event was less severe than the July 2006 EHE. We estimated that 20 extra deaths occurred during the August 2009 event. However, there were reductions for all four cases, and we calculated that approximately 10 lives would have been saved under case 1 and 4 mitigation scenarios, with slightly smaller reductions for cases 2 and 3.

As an initial step of investigating how important indoor exposure may be in determining heat-related morbidity and mortality, we supplement the conventional heat-mortality analysis above (which only includes outdoor exposure) with a cursory analysis of how heat mitigation strategies may alter individually experienced thermal environments. We then compare changes in outdoor exposure to changes in estimated exposure for the three studied subpopulations. Table 3 summarizes the EHH metric for five situations: outdoor conditions, the worst case of indoor conditions with windows always closed, and for individual exposures of the three

Fig. 6 Typical diurnal profiles for dew point temperature of **a**, elderly, **b** outdoor worker, and **c** office worker for July 24 of the 2006 heat event (first column) and August 29 of the 2009 heat event (second column)

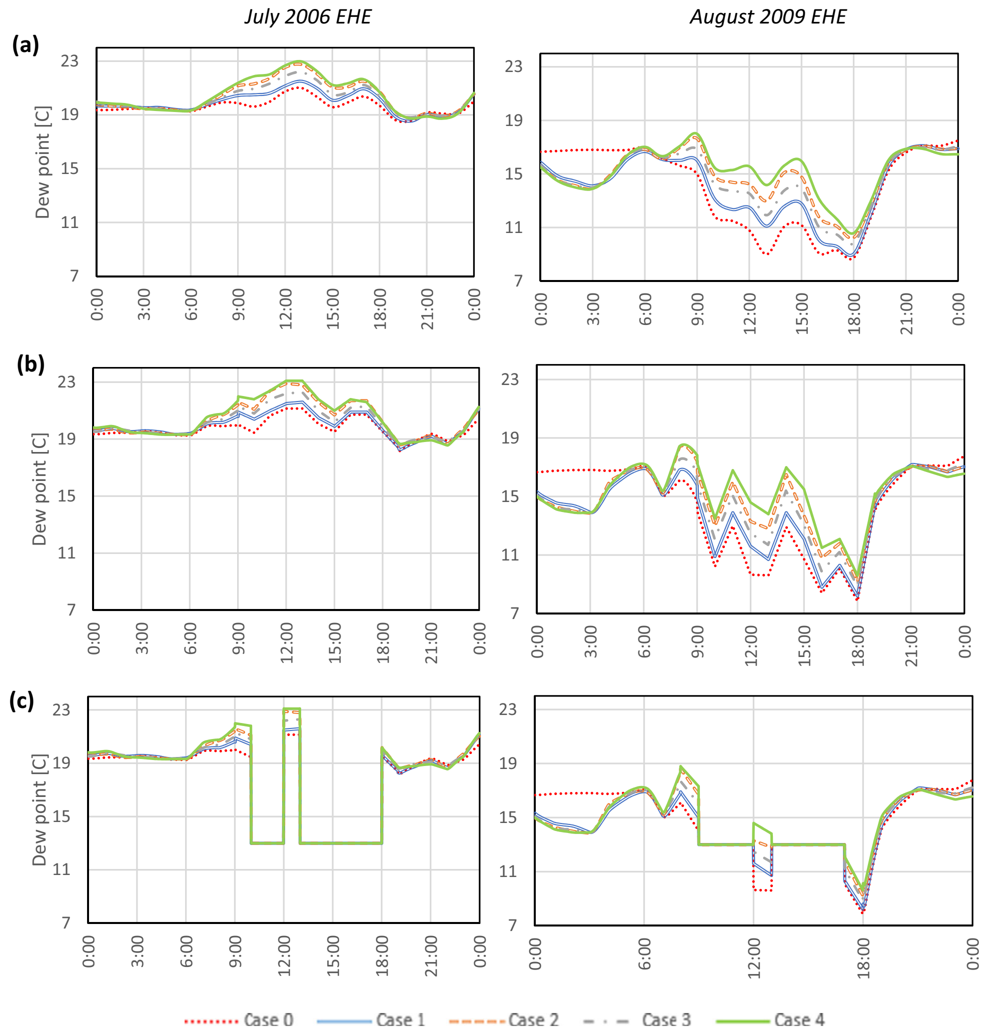

subpopulation groups based on behavior defined in Table 2. Results are presented for one representative day within each heat event. With respect to outdoor conditions, the 2006 event is clearly more oppressive than is the 2009 event. As noted earlier, the 2006 event resulted in a factor of 3 more estimated excess heat deaths than the 2009 heat event (60 vs. 20), using

Table 3 Excessive heat hours (degree-hours) of a typical day for each heat event and each simulation case. Results are presented for outdoor conditions, worst-case closed window indoor conditions, and the conditions experienced by each of the three population subgroups

Case	Description	Outdoor	Closed window indoor	Elderly	Office worker	Outdoor worker
July 2006 extreme heat event						
0	Control case	37.30	58.82	42.78	16.01	40.66
1	Low canopy, high albedo	28.46	46.85	33.97	12.56	31.12
2	High canopy, low albedo	37.20	58.37	43.15	14.73	40.10
3	Moderate canopy and albedo	33.35	53.43	39.27	13.85	36.43
4	High canopy and albedo	30.58	49.62	35.82	12.29	33.13
August 2009 extreme heat event						
0	Control case	12.09	16.97	11.96	2.89	12.15
1	Low canopy, high albedo	07.23	10.44	07.36	1.90	7.48
2	High canopy, low albedo	12.19	17.35	12.70	2.81	12.37
3	Moderate canopy and albedo	09.73	13.74	09.86	2.36	9.80
4	High canopy and albedo	09.33	13.80	09.98	2.27	9.49

the synoptic climatology modeling approach relating outdoor conditions to mortality. Interestingly, this corresponds quite well to the ratio of outdoor EHH for the control case (37.30 vs. 12.09, a factor of 3.1). It is clear from the first column in this table that the high albedo of case 1 results in the largest reduction in EHH for the outdoor environment—roughly a 24% and 40% reduction in EHH for the 2006 and 2009 heat events, respectively. Despite creating larger reductions in ambient air temperature, case 4, with its high albedo and high vegetation, was slightly less effective in reducing EHE than was case 1. This is due to the adverse effects on EHE of the increased humidity. The worst performing mitigation case, with respect to outdoor environments, was case 2 (low albedo and high canopy). While this case produced a slight reduction in EHE relative to the control case for the 2006 heat event, it actually increased EHE slightly in the 2009 event. These results clearly demonstrate the tradeoffs in outdoor conditions resulting from heat mitigation strategies that cool the ambient environment, but also increase dew point temperatures.

Table 3 also presents results for the closed window (worst case) indoor environment, and for each population subgroup. The general trends of decreasing EHH are consistent with those for the outdoor environment, with a few notable differences. First, a person confined to the (non-air-conditioned) indoor environment experiences heat exposures that are consistently 40–60% higher than a person continuously exposed to outdoor thermal conditions. With respect to control conditions, the elderly individual may experience total exposure (excessive heat hours—EHH) that are roughly the same (2009 event) or slightly worse (2006 event) than the outdoor worker. Of course, the office worker, who is assumed to spend the workday in an air-conditioned building, has a baseline exposure that is typically about 1/3 that of the other two population groups for all cases. As a result, the remainder of this discussion focuses on the elderly and outdoor worker subgroups, and on the more extreme case of the 2006 EHE. The high albedo case substantially reduced heat exposure for these groups. While case 1 reduced outdoor EHH for the 2006 event by 8.8 °C-h, the corresponding reductions in EHH were 8.8 and 9.5 °C-h for the elderly, and outdoor worker populations. So, for the elderly, the adverse effects of being confined to an indoor non-air-conditioned environment were offset by the reduction of heat flow through the roof due to the direct effects of the highly reflective roof surface. According to this analysis, the outdoor workers benefited more as they were not confined to an overheated building during the core hours of the day. However, it is crucial to recognize that the EHH metric used in assessing exposure assumes that outdoor exposures are in a shaded environment—and this is oftentimes not the case for outdoor workers. In contrast, for the case focused on increasing canopy cover (case 2), the EHH of the outdoor environment for the 2006 event decreased by 0.48 °C-h, while that for the elderly actually increased by 0.37 °C-h.

Discussion and conclusions

Measures of heat exposure and associated health risks of such exposures traditionally have focused on outdoor thermal conditions, despite the fact that urban residents spend the majority of their time inside buildings. In this study, we have used an excessive heat hours (EHH) metric as an indicator of risk for adverse health outcomes associated with outdoor and non-air-conditioned indoor exposures. We also characterized exposures for three distinct subpopulations: the elderly, indoor (office) workers, and outdoor workers. We found that in the absence of functioning air conditioning, the elderly have even higher exposure to extreme heat than do outdoor workers. While this only includes temperature and humidity, ignoring direct exposure to the sun, the finding makes it clear that studies of heat-health risks must account for the actual exposure pathways for different subpopulations in indoor and outdoor spaces.

In exploring the potential for heat mitigation strategies to reduce exposure (as measured by EHH), we found that, while mitigation focused on increasing vegetative cover can cool the urban environment, it also has adverse consequences due to the associated potential increase in dew point temperatures. However, heat mitigation that is accomplished through rooftop implementation of highly reflective roofing was found to produce similar neighborhood-level outdoor cooling while also directly benefiting the indoor environment through a reduction in the solar energy load on a building. Specifically, for the 2006 heat event, the high albedo low canopy cover scenario (case 1) reduced total EHH by about 9 °C-h for the elderly and outdoor worker populations. The high canopy cover, low albedo scenario (case 2), however, resulted in virtually no net impact on EHH due to the counteracting effects of decreased dry bulb temperatures and increased dew point temperatures.

These results strongly suggest that the more widespread use of reflective materials can mitigate both indoor and outdoor atmospheric conditions, and lessen the extent of negative health outcomes. While the levels of modification represented by each of the four test cases are aspirational, they are reflective of modification levels needed to achieve widespread urban cooling as outlined in Los Angeles' Sustainability pLAn. Additionally, the application of a synoptic climatological approach can assist in identifying those outdoor meteorological situations that are most stressful to an urban population. An important next step for modeling of heat-related health outcomes is to extend approaches such as this to account for both indoor and outdoor thermal exposures.

It should be noted that this analysis assumes uniform application of the high albedo and vegetative cover strategies across the entire city. Hence, we are not able to comment on scale effects associated with partial deployment of the strategies, or on the role that varying urban morphology across the city plays in the efficacy of the strategies. Furthermore, we ignore implementation and maintenance challenges, as well as potential unintended consequences (e.g., interaction of reflected shortwave radiation from paved surfaces with pedestrians and buildings).

References

[CDC] Centers for Disease Control and Prevention (2013) Heat illness and deaths–New York City, 2000-2011. MMWR Morb Mortal Wkly Rep 62:617–621

[NCHS] National Center for Health Statistics (2018) National Vital Statistics System, Centers for Disease Control and Prevention, http://web.archive.org/web/20181127154514/https://www.cdc.gov/nchs/nvss/deaths.htm Accessed 27 Nov. 2018

Akbari H, Rosenfeld AH, Taha H (1990) Summer heat islands, urban trees, and white surfaces. Lawrence Berkeley National Laboratory Report LBL-28308

Baniassadi A, DSailor DJ, Crank PJ, Ban-Weiss GA (2018) Direct and indirect effects of high-albedo roofs on energy consumption and thermal comfort of residential buildings. Energy Build 178(1):71–83

Chen F, Kusaka H, Bornstein R, Ching J, Grimmond CSB, Grossman-Clarke S, Loridan T, Manning KW, Martilli A, Miao S, Sailor D, Salamanca FP, Taha H, Tewari M, Wang X, Wyszogrodzki AA, Zhang C (2011) The integrated WRF/urban modeling system: development, evaluation, and applications to urban environmental problems. Int J Climatol 31:273–288

Crawley DB, Lawrie LK, Winkelmann FC, Buhl WF, Huang YJ, Pedersen CO, Strand RK, Liesen RJ, FIsher DE, Witte MJ, Glazer M (2001) EnergyPlus: Creating a new-generation building energy simulation program. Energy and Buildings 33:319–331

Fouillet A, Rey G, Laurent F, Pavillon G, Bellec S, Ghihenneuc-Jouyaux C, Clavel J, Jougla E, Hemon D (2006) Excess mortality related to the August 2003 heat wave in France. Int J Occup Environ Health 80:16–24

Garcetti E (2019) L.A.'s Green New Deal: Sustainable City pLAn, 151pp. https://plan.lamayor.org/. Accessed 28 May 2020

Hildebrandt EW, Bos W, Moore R (1998) Assessing the impacts of white roofs on building energy loads. ASHRAE Trans 104:810

Homer CG, Dewitz JA, Yang L, Jin S, Danielson P, Xian G, Coulston J, Herold ND, Wickham JD, Megown K (2015) Completion of the 2011 National Land Cover Database for the conterminous United States-representing a decade of land cover change information. Photogramm Eng Remote Sens 81(5):345–354

Kaiser R, Le Tertre A, Schwartz J, Gotway CA, Daley WR, Rubin CH (2007) The effect of the 1995 heat wave in Chicago on all-cause and cause-specific mortality. Am J Public Health 97(Suppl 1):S158–S162

Kalkstein AJ, Kalkstein LS, Vanos JK, Eisenman DP, Dixon PG (2018) Heat/mortality sensitivities in Los Angeles during winter: a unique phenomenon in the United States. Environ Health 17:1–12

Kalkstein LS, Klink F, Shickman K, Schneider S, Egolf M, Sailor D (2019) The potential impact of cool roof technologies upon heat wave meteorology and human health in Boston and Chicago. In: Roofing research and standards development, vol 9th. ASTM International, pp 1–27

King WJ, Klassen TP, LeBlanc J, Bernard-Bonnin AC, Robitaille Y, Coyle D, Tenenbein M, Pless IB (2001) The effectiveness of a home visit to prevent childhood injury. Pediatrics 108(2):382–388

Klepeis NE, Nelson WC, Ott WR, Robinson JP, Tsang AM, Switzer P, Behar JV, Hern SC, Engelmann WH (2001) The national human activity pattern survey (NHAPS): a resource for assessing exposure to environmental pollutants. J Expo Anal Environ Epidemiol 11(3):231–252

Krayenhoff ES, Moustaoui M, Broadbent AM, Gupta V, Georgescu M (2018) Diurnal interaction between urban expansion, climate change and adaptation in us cities. Nat Clim Chang 8:1097–1103

Kuras ER, Hondula DM, Brown-Saracino J (2015) Heterogeneity in individually experienced temperatures (IETs) within an urban neighborhood: insights from a new approach to measuring heat exposure. Int J Biometeorol 59(10):1363–1372

Kuras ER, Richardson MB, Calkins MM, Ebi KL, Hess JJ, Kintziger KW, Jagger MA, Middel A, Scott AA, Spector JT, Uejio CK, Vanos JK, Zaitchik BF, Gohlke JM, Hondula DM (2017) Opportunities and challenges for personal heat exposure research. Environ Health Perspect 125(8):085001

Lee S-H, Lee K-S, Jin W-C, Song H-K (2009) Effect of an urban park on air temperature differences in a central business district area. Landsc Ecol Eng 5:183–191

Mendon V, Lucas R, Goel S (2013) Cost-effectiveness analysis of the 2009 and 2012 IECC Residential Provisions–technical support document. U.S. Department of Energy Report PNNL-22068, 99pp https://doi.org/10.2172/1079749

Morini E, Touchaei AG, Rossi F, Cotana F, Akbari H (2018) Evaluation of albedo enhancement to mitigate impacts of urban heat island in Rome (Italy) using WRF meteorological model. Urban Clim 24:551–566

O'Lenick CR, Wilhelmi OV, Michael R, Hayden MH, Baniassadi A, Wiedinmyer C, Monaghan AJ, Crank PJ, Sailor DJ (2019) Urban heat and air pollution: a framework for integrating population vulnerability and indoor exposure in health risk analyses. Sci Total Environ 660:715–723

Oke TR (1976) The distinction between canopy and boundary-layer urban heat islands. Atmosphere 14(4):268–277

Pedersen CB (2015) Persons with schizophrenia migrate towards urban areas due to the development of their disorder or its prodromata. Schizophr Res 168:204–208

Rothfusz LP (1990) The heat index equation. National Weather Service Technical Attachment (SR 90–23)

Sailor DJ (1995) Simulated urban climate response to modifications in surface albedo and vegetative cover. J Appl Meteorol 34(7):1694–1704

Sailor DJ (1998) Simulations of annual degree day impacts of urban vegetative augmentation. Atmos Environ 32(1):43–52

Sailor DJ (2014) Risks of summertime extreme thermal conditions in buildings as a result of climate change and exacerbation of urban heat islands. Build Environ 78:81–88

Sailor DJ, Shepherd M, Sheridan S, Stone B, Kalkstein L, Russell R, Vargo J, Andersen T (2016) Improving heat-related health outcomes in an urban environment with science-based policy. Sustainability 8(10):1–13

Salamanca F, Martilli A, Yagüe C (2012) A numerical study of the urban heat island over Madrid during the DESIREX (2008) campaign with WRF and an evaluation of simple mitigation strategies. Int J Climatol 32:2372–2386

Santamouris M (2014) Cooling the cities-a review of reflective and green roof mitigation technologies to fight heat island and improve comfort in urban environments. Sol Energy 103:682–703

Semenza JC, Rubin CH, Falter KH, Selanikio JD, Flanders WD, Howe HL, Wilhelm JL (1996) Heat-related deaths during the July 1995 heat wave in Chicago. N Engl J Med 335:84–90

Shen H, Tan H, Tzempelikos A (2011) The effect of reflective coatings on building surface temperatures, indoor environment and energy consumption—an experimental study. Energy Build 43(2–3):573–580

Sheridan SC, Kalkstein LS (2004) Progress in heat watch-warning system technology. Bull Am Meteorol Soc 85:1931–1941

Sheridan SC, Kalkstein AJ, Kalkstein LS (2009) Trends in heat-related mortality in the United States, 1975-2004. Nat Hazards 50:145–160

Stone B, Vargo J, Habeeb D (2012) Managing climate change in cities: will climate action plans work? Landsc Urban Plan 107(3):263–271

Vassos E, Agerbo E, Mors O, Pedersen CB (2016) Urban-rural differences in incidence rates of psychiatric disorders in Denmark. Br J Psychiatry 208:435–440